Mechanisms of Inter-ply Void Formation during Vacuum Bag-only Cure of Woven Prepregs

Wei Hu*, Timotei Centea, Steven Nutt

M.C. Gill Composites Center, Department of Chemical Engineering and Materials Science, University of Southern California, 3651 Watt Way VHE-602, Los Angeles, CA 90089-0241, USA

* E-mail: weihu@usc.edu

Abstract

The removal of inter-ply air is critical for limiting porosity in laminates. In this study, an *in situ* monitoring technique was employed to observe inter-ply air evolution during vacuum bag-only cure. Observations showed that reduced vacuum resulted in inefficient inter-ply air evacuation, a more rapid bubble expansion rate, and formation of new air bubbles. A modified tow impregnation model showed that resin infiltration was impeded at reduced vacuum conditions due to the presence of intra-tow air. However, the cured laminates showed that tows were fully impregnated in all cases, indicating that the entrapped intra-tow air migrated to inter-ply regions during cure. The interactions between intra-tow and inter-tow air at deficient vacuum conditions were revealed. Findings led to the conclusion that air remaining in intra-tow regions contributed more to the increase of inter-ply voids than the reduction in consolidation pressure difference associated with reduced vacuum.

Key words: fabric prepreg, inter-ply voids/ porosity, out of autoclave processing, reduced vacuum.

1. INTRODUCTION

Please cite the article as: W. Hu, Timotei Centea, Steven Nutt, **"Mechanisms of Inter-ply Void Formation during Vacuum Bag-only Cure of Woven Prepregs,"** *Polymer Compos* (2019) DOI

Vacuum bag-only (VBO) processing of prepreg is an appealing out-of-autoclave technique for the manufacture of high-performance composite parts [1]. Advantages over autoclave processing include the reduction of capital and operational costs, greater energy efficiency, increased throughput, and removal of size limits. However, because the maximum pressure in VBO processing is only 0.1 MPa (1 atm), VBO-cured parts can sometimes exhibit unacceptable levels of porosity, and diminished mechanical properties [2–4]. Thus, defect control is critical to the successful transition from autoclave processing to out-of-autoclave processing.

Entrapped air and moisture are two primary sources of void formation. To promote air evacuation, the initial microstructure of VBO prepregs contains an interconnected network of dry, unimpregnated regions, known as engineered vacuum channels (EVaCs) [5]. When vacuum is applied, these EVaCs facilitate air evacuation through edge-breathing dams at the periphery of the laminate. Upon heating, resin viscosity decreases, and the dry fiber tows are infiltrated and saturated (ideally) by surrounding resin to produce a void-free laminate. Although the design of dry fiber regions allows more efficient in-plane air evacuation, it also adds complexity to the VBO consolidation process, which involves gas flow, resin flow and void formation, all of which are likely to interact during cure. In practice, air can be trapped between prepreg plies during layup as well as in the dry fiber tow regions if it is isolated during the resin infiltration process.

Previous studies have shown that variations in material properties and processing conditions can have adverse effects on final part quality [6–11]. For example, Grunenfelder and Nutt reported that final void contents increased with increasing moisture content in VBO-cured parts, while autoclave-cured parts remained void-free in all conditions [6]. They also investigated the effects of room-temperature out-time on part quality and concluded that significant tow porosity occurred when the out-time exceeded the material out-life specification [7]. Centea and

Hubert assessed the effects of three pressure-related process deficiencies on consolidation and part quality [8]. They showed that the process deficiencies led to specific void content levels, distribution and morphologies, and were more pronounced in woven fabric prepregs. These studies established the basic material - process - quality relationships. However, the precise mechanisms of void formation and growth during cure in prepreg composites are not yet fully understood [12].

Transparent glass tooling surfaces have been employed in previous studies to observe air entrapment, distribution and resin flow *in situ* [13–15]. This technique can provide valuable insight into void evolution and transport during processing. In previous work, we reported an *in situ* monitoring technique that allowed real-time observations of the evolution of inter-ply voids during cure [16]. By incorporating a perforated resin film between a glass tool plate and a stack of prepreg plies, we introduced air bubbles with controlled size and distribution into the layup, mimicking the conditions surrounding an internal void located in the resin-rich regions between prepreg plies. This technique was used to identify mechanisms of void formation and removal in unidirectional prepregs, and to address the effects of key processing parameters on void evolution, providing insights into bubble migration, expansion, and removal during cure [16,17].

The present work aims to improve understanding of void evolution in fabric prepregs and to clarify the effects of reduced vacuum on void evolution, including the underlying mechanisms. We employed the same *in situ* monitoring method to investigate mechanisms of inter-ply void evolution in fabric prepregs. First, void evolution during cure at standard conditions (full vacuum) was studied to establish inter-ply air removal mechanisms. Then, the effects of reduced vacuum on each stage of void evolution were investigated to understand void formation and removal mechanisms during each stage. Tow impregnation during cure at reduced vacuum conditions was also studied, and a tow impregnation model was modified to provide insights into the effects of

reduced vacuum on resin infiltration. Finally, based on the observations and model predictions, the interactions between intra-tow air and inter-ply air at reduced vacuum conditions were addressed.

2. EXPERIMENTAL PROCEDURE

2.1. Materials

The material selected for this study was a carbon fiber-epoxy prepreg formulated for vacuum bag-only cure. The prepreg consisted of an eight-harness satin (8HS) fabric (T650-35, 3K) and a toughened epoxy resin (CYCOM 5320-1, Solvay). Neat resin film (CYCOM 5320-1, Solvay) was also used, with areal weight ~ 92 g/m^2 and thickness ~50 µm. The single-dwell cure cycle was 93°C for 12 h, with an average ramp rate of ~2°C/min. To investigate the effects of vacuum quality on void evolution, laminates were fabricated using full vacuum, 80% vacuum (corresponding to an absolute bag pressure of ~20.3 kPa) and 70% vacuum (corresponding to an absolute bag pressure of ~30.4 kPa). The bag pressure was monitored throughout cure using a pressure sensor or a vacuum gauge.

2.2. *In Situ* Monitoring of VBO Cure

To observe air evacuation and entrapment during VBO cure, a custom-built experimental setup was used, incorporating *in situ* visual observation. A perforated resin film was laid up against the glass window of an oven, followed by four layers of prepreg plies and standard consumables, shown in Figure 1. The perforated resin film was fabricated by punching holes into the neat resin film using a coring tool with a diameter of 0.25 mm and spacing between holes of 2 mm. The resin film was introduced into the lay-up to replicate the conditions of air bubbles that are trapped in the resin during resin preparation and/or between prepreg plies during the lay-up process. For the test panels, prepreg plies were cut to 127 × 127 mm, while the perforated resin film was 38 × 38 mm.

Each laminate consisted of four plies stacked $[0/90]_2$ and was cured in a programmable air-circulating oven (Thermal Products Solution Blue M). Temperature was measured by two thermocouples on the glass side throughout the cure cycle. Time-lapse videos were recorded throughout the cure using a portable microscope (Dino-Lite Premier 2 Digital Microscope) with a magnification of 20.

2.3. Void Content

Void content as a function of time was measured for each *in situ* monitoring test panel. Ten representative images were selected from the time-lapse video for subsequent analysis. The area where the prepreg was not in contact with the perforated resin film was considered as voids. Voids in the images (with an area of ~20 mm × 16 mm) were manually selected and converted to binary, and void content, size, and number of voids were calculated using image analysis software (ImageJ). Void content was determined as the ratio of the area of voids to the total area.

2.4. Model Development

Tow impregnation is a key flow process occurring during VBO prepreg cure. Models have been developed to predict the flow kinetics, in light of various material properties and process parameters [7,18–20]. In this study, a simple approach previously developed by Centea et al. [19] was modified to capture the effects of vacuum conditions on tow impregnation. The model is based on Darcy's Law for the low Reynolds number infiltration of a viscous fluid within a porous medium and mass continuity:

$$\bar{v} = -\frac{\bar{\bar{K}}}{\mu(1-V_s)}\nabla P \quad (1)$$

$$\nabla \cdot \bar{v} = 0 \quad (2)$$

In Eqs. (1) and (2), $\bar{v}$ is the average velocity of the fluid within the pores; $\bar{\bar{K}}$ is the permeability tensor of the medium; μ is the dynamic viscosity of the fluid; V_s is the volume fraction of the solid; and P is the fluid pressure. The framework can be simplified by assuming that (a) the dry fiber bed regions ahead of the resin flow front are compressed to a constant volume fraction V_f, (b) the tows are circular, and (c) the flow front is axisymmetric within the cross-section and uniform along the tow length. With the radius of the tow being R_{tow}, the radius of the resin flow front being R_f, and the corresponding resin pressure boundary conditions being P_∞ and P_f, respectively, Eqs. (1) and (2) were combined to obtain the following expression for the resin flow front velocity:

$$v_f = \frac{dR_f}{dt} = -\frac{K}{\mu(1-V_f)}\left(\frac{1}{R_f}\frac{(P_f-P_\infty)}{ln(R_f/R_{tow})}\right) \quad (3)$$

By defining a degree of impregnation β ($0 \leq \beta \leq 1$), Eq. (3) can be normalized to obtain the tow impregnation model:

$$\beta = 1 - \frac{R_f}{R_{tow}} = 1 - \sqrt{\frac{A_f}{A_{tow}}} \quad (4)$$

$$\frac{d\beta}{dt} = \frac{K}{\mu R_{tow}^2(1-V_f)}\left(\frac{P_\infty - P_f}{(1-\beta)ln(1/(1-\beta))}\right) \quad (5)$$

Eq. (5) can be used to predict the evolution of the degree of tow impregnation of the prepreg for any time-temperature cycle, provided the following parameters are determined: the evolution of the resin viscosity μ; the tow volume fraction and geometry; the pressure boundary condition P_∞ and P_f, and the tow transverse permeability, K.

The dynamic viscosity μ of the resin was determined using the predictive models developed by Kim et al. [21]. Tow properties were determined according to the method described

in Ref. [19]. A fiber volume fraction of $V_f = 0.74$ was used for the 8HS prepregs. The major and minor diameters of the elliptic tows were 2.44 mm and 0.33 mm, measured from an average of 20 tow cross-sections. These values were converted to an equivalent circular tow radius of 0.116 using the relation proposed by Van West et al. [22], who reported that circles and ellipses with equal hydraulic radii have the same fill times. The tow permeability K was a constant and was obtained from [7]. The values of all the constants are listed in Table 1.

The pressure boundary condition P_∞ at $r = R_{tow}$ is assumed to be the atmospheric pressure, while the pressure boundary condition at P_f at $r = R_f$ is assumed to be the difference between the gas pressure entrapped within the tow P_{gas} and the capillary pressure P_c:

$$P_f = P_{gas} - P_c \tag{6}$$

Here, because the test panels were small and flat, the initial gas pressure P_{gas} within the tow was assumed to be the same as the bag pressure P_{vac}. Thus, $P_{gas} = 0$ throughout the cure under perfect vacuum conditions, while under reduced vacuum conditions, gas pressure during cure is more complex, and can be affected by the rate of air transport out of the part, temperature, and degree of impregnation. Although the exact evolution of P_{gas} was unknown, in principle, air within fiber tows can be driven out by the infiltrating resin until no continuous pathways remain in the tows.

To a first approximation, the evolution of P_{gas} was separated into two stages by introducing a critical degree of tow impregnation β_c. We assumed that before the degree of impregnation reaches β_c, air within the tow can evacuate instantaneously, a constant vacuum pressure condition $P_{gas} = P_{vac}$ can be applied at the resin front, while once the degree of impregnation exceeds β_c, gas inside the tow can no longer be evacuated (i.e., the mass of the gas inside the tow remains constant). Upon reaching β_c, P_{gas} can be updated using the ideal gas law. Here, $\beta_c = 0.8$ was used,

because experiments showed that the effective in-plane air permeability decreased by two orders of magnitude when the degree of impregnation reached 0.8 (from 4.44E-14 m^2 to 4.49E-16 m^2 for this material). With all parameters defined, Eq. (5) can be solved using a forward-Euler linear solver over small time steps (Δt = 1s) to predict the evolution of β during cure.

2.5. Degree of Impregnation During Cure

To compare the model predictions with experimental data, laminates were partially processed to selected points during the temperature ramp of the prepreg cure cycle (75°C, 80°C and 85°C) under different vacuum conditions. Subsequently, panels were removed from the oven and rapidly quenched to room temperature to prevent further resin flow. The partially cured laminates were then cold-cured in an ammonia environment at room temperature for a week (following the protocol described by Howard [23]) to achieve a hard and stiff structure while preserving the morphology of the laminates at each point of interest. Samples were sectioned at the center of each panel, polished, and inspected using a stereo microscope (Keyence VH-Z100R). For each sample, 20 individual tow cross-sections were manually selected. The visible dry fiber tow area A_f, as well as the total area of the fiber tow A_{tow}, was measured using ImageJ. The degree of impregnation β was obtained by Eq. (4).

3. RESULTS AND DISCUSSION

3.1. Inter-ply Air Removal During VBO Cure

The evolution of air entrapped in the resin-rich inter-ply regions is shown in Fig. 2. Initially, air was trapped both in the artificial pores (Fig. 2a, circled in red), and between the perforated resin film and the first prepreg ply (Fig. 2a, white regions). The naturally trapped air pockets in 8HS prepreg were patterned and continuous, corresponding to the woven fiber-bed

architecture; most of the trapped air accumulated in the gaps between the resin film and depressed regions of the fabric. Once vacuum was applied, air evacuated rapidly through the pinholes at the intersections of warp and weft tows. Ten minutes after the application of vacuum, the majority of both artificial bubbles and naturally trapped air were removed (Fig. 2b), indicating that most inter-ply air can be evacuated effectively at a relatively low temperature. As temperature increased, air bubbles began to migrate alongside fiber tows towards the pinholes, achieving further air evacuation. At ~80°C, only a few small air bubbles remained, and the overall void content declined to a minimum value (Fig. 2c). Following this point in the cure cycle, in accordance with void evolution in UD prepregs [16], the remaining air bubbles increased in size for ~ 25 minutes. Then, the bubbles gradually shrank throughout the remainder of the cure cycle. Most air bubbles were removed by the end of the cure cycle, resulting in a nearly void-free laminate (Fig. 2f).

Fig. 3a shows the relationship between resin properties, tow impregnation, and void content. As reported previously [16], void evolution in *UD* prepregs can be divided into three stages based on the correlation of bubble behavior, resin properties and tow impregnation . For *fabric* prepregs studied here, all three stages were observed, indicating that the dominant mechanisms of void evolution remained unchanged. The three stages, denoted with Roman numerals in Fig. 3a, include (I) air evacuation, (II) bubble expansion and (III) bubble shrinkage. During Stage I, as resin viscosity remains relatively high, and fiber tows are partially saturated, inter-ply air is evacuated from the resin-starved regions at the intersections of fiber tows. Fig. 3b shows the distribution of resin on the uncured prepreg surface. The open slits (dark areas) located around almost every intersection of fiber tows provide pathways for air to quickly evacuate through dry fiber tows to a breathing edge.

During Stage II, resin viscosity is near a minimum, and dry fiber tows are almost fully

impregnated. The increase in void size during this stage is attributed to moisture diffusion from the prepreg resin to the air bubbles [16]. Because water vapor pressure increases exponentially with increasing temperature, when the water vapor pressure within the voids exceeds the local surrounding resin pressure, voids grow [15]. Finally, during Stage III, the occurrence of bubble shrinkage is attributed to the increase of water solubility with increasing degree of cure and the decrease in total water content in the prepreg as cure proceeds [16]. Both phenomena are expected to reverse the direction of moisture diffusion from air bubbles to resin.

3.2. Effects of Reduced Vacuum on Void Evolution During Cure

Fig. 4a shows void content of prepregs during cure under reduced vacuum conditions. For all tests, the initial void content was ~ 50%. At the end of Stage I, the average void content of prepregs at 70% and 80% vacuum decreased to ~ 1.2% and ~ 0.9%, respectively. Both porosity levels were slightly greater than that of the control panel (~ 0.7%), indicating that air evacuation in fabric prepregs became less efficient under reduced vacuum conditions. At ~ 80°C, bubble expansion occurred roughly in the same manner as in the control panel. However, the duration of Stage II (bubble expansion) at 80% vacuum extended to 4 hours, and by the end of Stage II, the void content increased to ~ 1.2% (30% greater than control panel). Similar behavior was observed in UD prepregs, although the duration of Stage II was only ~ 30 minutes longer than the control [17]. The increased void content was attributed to the decrease in consolidation pressure difference, as well as the associated change in local resin pressure resulting from reduced vacuum [18].

At 70% vacuum, surprisingly, Stage III (bubble shrinkage) was not observed throughout the cure cycle. A minimum value was reached at the end of Stage I, after which the void content

increased steadily until gelation. These observations indicate that further reducing vacuum level will strongly affect the post-removal growth / shrinkage mechanisms (Stage II and Stage III). The final void content of prepreg at 80% vacuum was ~1% (10 times greater than control panel), while that at 70% vacuum was ~ 2%.

To obtain a clearer picture of void evolution, the average bubble size and number of bubbles during cure were investigated for all three vacuum conditions (see Fig. 4b). Because the naturally trapped air pockets were interconnected at the outset, the initial size and number of bubbles were not calculated, and Stage I was not included. Stages II and III were divided based on the void evolution of the control panel. The plot shows that both size and number of bubbles increased with decreasing vacuum at most of the junctures measured throughout the cure. At full vacuum, bubble size nearly doubled during Stage II, then decreased slightly during Stage III, while the number of bubbles decreased throughout the cure. At 80% vacuum, bubble size increased steadily until 4 hours into the cure cycle, while the number of bubbles gradually decreased throughout the cycle. At 70% vacuum, the bubble size increased markedly from ~ 45 minutes to 1 hour into the cure cycle. The number of bubbles also decreased rapidly during the same period, indicating that air was evacuating, most likely due to a delay in resin infiltration. After that, both size and number of bubbles increased gradually until gelation, indicating that new bubbles formed during Stage III, which was not observed at full vacuum.

Based on these observations, the effects of reduced vacuum on inter-ply void evolution include (1) less efficient inter-ply air evacuation during Stage I due to the lower pressure gradient between inter-ply regions and vacuum source, (2) increased bubble expansion time and expansion rate during Stage II, attributed to the decrease in consolidation pressure differential and local resin pressure, and (3) formation of new air bubbles during Stage III, indicating a new source of voids at

reduced vacuum conditions (discussed later). In addition, reduced vacuum can impede tow impregnation due to the resistance of residual air in dry fiber tows.

3.3. Effects of Reduced Vacuum on Air Evacuation

To investigate the effects of reduced vacuum on air removal during Stage I and the effects of inefficient initial air evacuation on void evolution, a 2-hour vacuum hold (unheated) was performed prior to cure at 70% and full vacuum. Fig. 5a shows void content as a function of time during room temperature vacuum hold. During the first 15-minute vacuum hold at full and 70% vacuum, the void content decreased from ~ 50%, to ~ 8% and ~ 15%, respectively. At the end of the vacuum hold, however, the void content in both cases decreased to a similar value (~ 3%), indicating that although the inter-ply air removal process was slower at reduced vacuum, most inter-ply air bubbles could be evacuated with sufficient vacuum hold time.

Fig. 5b shows the void content during the subsequent heated cure. As temperature increased, additional air evacuation occurred in both cases. At the end of Stage I, void contents for the prepregs cured at full-vacuum and at 70% vacuum decreased to ~ 0.4% and to ~ 0.7%, respectively. Both void levels were less than the control panel cured at full vacuum without an unheated vacuum hold. The void content in prepreg cured at full vacuum reached a plateau during Stage II, then gradually decreased. Further observation of the *in situ* video showed that the remaining air bubbles expanded slightly during Stage II and shrank gradually during Stage III, and no bubble formation was observed after Stage I. However, the void content of the prepreg at 70% vacuum increased steadily and exhibited a marked increase in bubble size, and new bubbles formed as well. The final void content of the prepreg at 70% vacuum was ~ 1.5%, roughly twice the porosity in the control panel.

The findings indicate that while the unheated vacuum hold under deficient vacuum can reduce the amount of initial inter-ply air to the same extent as that at full vacuum, the vacuum hold has little influence on reducing defect contents in the final laminates. In other words, the inefficient evacuation of inter-ply air bubbles during Stage I is not the major cause of the high final void content at reduced vacuum conditions. We hypothesize that the final inter-ply void content is determined by residual air remaining in the prepreg assembly (both inter-tow and intra-tow) when the prepreg is fully saturated.

3.4. Effects of Reduced Vacuum on Bubble Expansion

As discussed in Section 3.2, the longer bubble expansion time and higher expansion rate observed at reduced vacuum levels were hypothesized to result from the reduced consolidation pressure difference. Specifically, these observations were attributed to the associated change in local resin pressure as bubbles expand when the internal gas pressure exceeds the surrounding resin pressure and surface tension. To test this hypothesis, two experiments were performed by controlling vacuum level during different stages of cure. As shown in Fig. 6, the vacuum history for the red curve was full vacuum during the Stage I - the vacuum level was changed at the end of Stage I (red arrow), when temperature reached 80°C, followed by 70% vacuum during the remainder of the cure. Compared to a control panel cured at full vacuum (the blue curve), the bubble expansion rate for the red curve was slightly greater, and the final void content was also greater, confirming that reduced vacuum level affects the bubble expansion process. However, all three stages were manifest in the red curve, and the final void content was much less than that at 70% vacuum. The findings indicate that reducing vacuum level during Stages II and III does not substantially affect the bubble expansion/ shrinkage mechanisms.

In contrast, the black curve in Fig. 6 shows a vacuum history that began with 70% vacuum during the Stage I, followed by full vacuum. After increasing to full vacuum (red arrow), void contents continued to fall for about 20 minutes, then increased steadily for the remainder of the cure cycle. Although full vacuum was applied during Stages II and III, the final void content was similar to that at 70% vacuum, indicating that moisture vaporization was not the sole source of bubble expansion. Failure to maintain a high vacuum quality at the beginning of the cure could cause significantly increased porosity.

3.5. Effects of reduced vacuum on tow impregnation

To understand the influence of reduced vacuum on intra-tow air entrapment and resin infiltration, a model was modified (described in Section 2.4), and the model results were compared to experimental data. Fig. 7a shows the model predictions for degree of impregnation as a function of temperature and time at different vacuum levels. The model predictions show that tow impregnation rate decreases with decreasing vacuum level. The measured data (shown in Fig. 7b) also show that the infiltration process decelerates as vacuum level decreases. The model predictions match the experimental data during the tow impregnation process, indicating that the model captures the key effects of reduced vacuum on tow impregnation.

Model predictions also show that for prepreg cured at 70% and 80% vacuum, resin infiltration ceases before full tow impregnation due to the presence of intra-tow entrapped air. However, cross-sections of the cured laminates (Fig. 8) show that fiber tows were fully impregnated in all three vacuum conditions, contrary to the model predictions. One possible reason for the difference is that air is fully evacuated before tow impregnation is completed in all three conditions. However, this explanation is unlikely to be valid at reduced vacuum conditions, as tow

impregnation during cure is not uniform. When fiber tows are highly impregnated and dry fiber regions become isolated, air can no longer be evacuated. A second (more likely) possible explanation of the difference between model predictions and experimental data is that trapped intra-tow air migrates into inter-ply regions during cure, which the model does not account for. Figs. 8 (a-c) show that inter-tow voids increased with decreasing vacuum level, an indication of a potential interaction between intra-tow air and inter-ply voids. To confirm this hypothesis, an additional panel was cured at 100% vacuum with sealed edges to ensure air was trapped in the dry fiber tows during cure. Fig. 8d shows that in this case, most fiber tows were still fully impregnated, and large voids appeared in inter-ply regions, supporting the assertion that air trapped in the dry fiber tows can migrate to inter-ply regions as resin infiltrates the tows.

3.6. The Interaction Mechanisms – Inter-ply Voids and Intra-tow Air

Based on the *in situ* tests described above, three main interactions between inter-ply air bubbles and the trapped intra-tow air were identified (Fig. 9). Figs. 9 (a-c) show that at 70% vacuum, inter-ply air bubble size increased steadily throughout the cure, starting from the end of Stage I. This observation confirms that the higher expansion rate and longer expansion time at reduced vacuum conditions are caused not only by moisture diffusion, but also the coalescence of intra-tow and inter-ply air bubbles.

Figs. 9 (d-f) show that a bubble emerged from a tow intersection (arrow) at 50 minutes into the cure, and developed into a large air bubble within 5 minutes. This observation was not an isolated case, but was observed repeatedly in both 70% and 80% vacuum conditions, despite the small field of view of the microscope. Moreover, those bubbles appeared at roughly the same time that tow impregnation was entering the plateau region of the model predictions, i.e., when the resin flow front could no longer infiltrate remaining dry fiber regions. This change in boundary

condition could strongly affect the microstructure of the laminate, potentially changing the local pressure gradient and causing air bubbles near pinholes to migrate from fiber tows to resin-rich regions. Studies have shown that there is an increase in gas mobility when resin viscosity decreases to its minimum [24,25], which promotes air migration. Furthermore, air migration can reduce surface tension of air bubbles when elongated shapes, typically constrained by fiber arrays, adopt spherical shapes in resin-rich regions.

Figs. 9 (g-i) show an elongated air bubble formed alongside adjacent fiber tows in prepreg cured at 70% vacuum. Unlike the second type of bubble formation, the onset of this expansion occurred at ~ 90 minutes into cure, and expansion was a slow process, lasting several hours. Furthermore, this kind of air bubbles was observed only in prepregs cured at 70% vacuum. As the vacuum level further decreased, fiber tows underwent less compaction, and the trapped intra-tow air gradually migrated to inter-ply regions directly through fiber tows.

4. CONCLUSIONS

Degradation of composite mechanical properties often correlates with porosity, as well as the shape, size and locations of the voids. Failure typically initiates from large voids located in resin-rich inter-ply regions, especially for matrix dominant properties [26,27]. A thorough understanding of the formation mechanisms and evolution of inter-ply voids is key to building a basis for science-based defect reduction strategies. The present work provides new insights into void evolution during VBO cure of prepregs, and the effects of reduced vacuum on inter-ply void formation. These insights are provided largely through the development and use of an *in situ* monitoring technique.

Most studies have argued that the increase in void content under deficient vacuum conditions is a result of decreased consolidation pressure. However, we conclude that the sharp

increase in both size and number of inter-ply air bubbles under such conditions arises because of the remaining intra-tow air, rather than the reduced consolidation pressure. Our results also show that even full vacuum is not sufficient to prevent the migration of intra-tow air towards the inter-ply regions if air remains in the prepreg system at the end of Stage I. These new insights emphasize strict control of vacuum quality, especially during the early stage of cure. In addition, they also highlight the need for sufficient air evacuation *prior to* tow saturation. Air evacuation in VBO prepregs (with conventional formats) can be especially challenging for large parts and/or those with complex geometries, as it relies almost entirely on edge-breathing. To increase the efficiency of air evacuation in VBO prepregs, modified prepreg formats with shorter breathe-out pathways may be helpful to mitigate this issue [28,29].

Note that in our previous work, interactions between intra-tow and inter-tow air were *not* observed during the cure of unidirectional prepregs at 80% vacuum [17], indicating that these interactions are also affected by the fiber bed architecture. The inherent waviness of woven fiber tows and the presence of resin-rich pinholes could promote migration of intra-tow air due to the potential change in local pressure gradient. Thus, prepregs with less tow intersections such as unidirectional tape and spread tow fabric might be less susceptible to vacuum deficiencies.

The transition from autoclave processing towards out-of-autoclave processing may rely on the ability to replace the process robustness that autoclave pressures provide, and instill characteristics into OoA prepregs that restore some of that robustness. This task will require both optimization of OoA prepreg formats and process parameters to minimize porosity. This study provides new insights into mechanisms of air removal at reduced vacuum conditions during cure of OoA prepregs, which can guide the design of prepregs and processes to restore process robustness to OoA cure. Furthermore, the *in situ* monitoring method employed here can be applied

more widely to assess void formation mechanisms and bubble behavior during cure, as well as for parametric studies with various prepreg formats.

Acknowledgements: The authors acknowledge Solvay Group (Scott Lucas, Steve Howard) for the donation of the prepreg and resin film used in this work and Airtech International Inc. (Cole Standish) for the consumables. The work was supported by the M.C. Gill Composites Center.

References:

1. Centea T, Grunenfelder LK, Nutt SR. A review of out-of-autoclave prepregs - Material properties, process phenomena, and manufacturing considerations. Compos Part A Appl Sci Manuf 2015;70:132–54. doi:10.1016/j.compositesa.2014.09.029.
2. Zhan-Sheng Guo, Ling Liu, Bo-Ming Zhang, Shanyi Du. Critical Void Content for Thermoset Composite Laminates. J Compos Mater 2009;43:1775–90. doi:10.1177/0021998306065289.
3. Liu L, Zhang BM, Wang DF, Wu ZJ. Effects of cure cycles on void content and mechanical properties of composite laminates. Compos Struct 2006;73:303–9. doi:10.1016/j.compstruct.2005.02.001.
4. Bowles KJ, Frimpong S. Void Effects on the Interlaminar Shear Strength of Unidirectional Graphite-Fiber-Reinforced Composites. J Compos Mater 1992;26:1487–509. doi:10.1177/002199839202601006.
5. Centea T, Hubert P. Measuring the impregnation of an out-of-autoclave prepreg by micro-CT. Compos Sci Technol 2011;71:593–9. doi:10.1016/j.compscitech.2010.12.009.
6. Grunenfelder LK, Nutt SR. Void formation in composite prepregs - Effect of dissolved moisture. Compos Sci Technol 2010;70:2304–9. doi:10.1016/j.compscitech.2010.09.009.
7. Grunenfelder LK, Centea T, Hubert P, Nutt SR. Effect of room-temperature out-time on tow impregnation in an out-of-autoclave prepreg. Compos Part A Appl Sci Manuf 2013;45:119–26. doi:10.1016/j.compositesa.2012.10.001.
8. Centea T, Hubert P. Out-of-autoclave prepreg consolidation under deficient pressure conditions. J Compos Mater 2014;48:2033–45. doi:10.1177/0021998313494101.
9. Anderson JP, Altan MC. Formation of Voids in Composite Laminates : Coupled Effect of Moisture Content and Processing Pressure. Polym Compos 2015;36:376–84. doi:10.1002/pc.
10. Wells J, Kay J, Poursartip A, Lane M, Fernlund G. Surface and Bulk Porosity in Out-of-Autoclave Prepregs. Proc. Int. Conf. Compos. Mater. (ICCM-20). Copenhagen, Denmark July 19-24, 2015, p. 12.
11. Préau M, Hubert P. Effects of processing conditions on bondline void formation in vacuum bag only adhesive bonding : Modelling , validation and guidelines. Int J Adhes Adhes 2018;80:43–51. doi:10.1016/j.ijadhadh.2017.10.004.
12. Mehdikhani M, Gorbatikh L, Verpoest I, Lomov S V. Voids in fiber-reinforced polymer composites: A review on their formation, characteristics, and effects on mechanical performance. J Compos Mater 2018:002199831877215. doi:10.1177/0021998318772152.
13. Cender TA, Simacek P, Advani SG. Resin film impregnation in fabric prepregs with dual length scale permeability. Compos Part A Appl Sci Manuf 2013;53:118–28.

doi:10.1016/j.compositesa.2013.05.013.
14. Hamill L, Centea T, Nutt S. Surface porosity during vacuum bag-only prepreg processing: Causes and mitigation strategies. Compos Part A Appl Sci Manuf 2015;75:1–10. doi:10.1016/j.compositesa.2015.04.009.
15. Helmus R, Kratz J, Potter K, Hubert P, Hinterholzl R. An experimental technique to characterize interply void formation in unidirectional prepregs. J Compos Mater 2017;51:579–91. doi:10.1177/0021998316650273.
16. Hu W, Grunenfelder LK, Centea T, Nutt S. In-situ monitoring of void evolution in unidirectional prepreg. J Compos Mater 2018;52:2847–58. doi:10.1177/0021998318759183.
17. Hu W, Nutt S. In-situ Montoring of Air Removal During Vacuum Bag-Only (VBO) Processing. 21st Int. Conf. Compos. Mater., Xi'an, 20-25th, 2017: n.d.
18. Helmus R, Centea T, Hubert P, Hinterholzl R. Out-of-autoclave prepreg consolidation: Coupled air evacuation and prepreg impregnation modeling. J Compos Mater 2016;50:1403–13. doi:10.1177/0021998315592005.
19. Centea T, Hubert P. Modelling the effect of material properties and process parameters on tow impregnation in out-of-autoclave prepregs. Compos Part A Appl Sci Manuf 2012;43:1505–13. doi:10.1016/j.compositesa.2012.03.028.
20. Kourkoutsaki T, Comas-Cardona S, Binetruy C, Upadhyay RK, Hinterhoelzl R. The impact of air evacuation on the impregnation time of Out-of-Autoclave prepregs. Compos Part A Appl Sci Manuf 2015;79:30–42. doi:10.1016/j.compositesa.2015.08.034.
21. Kim D, Centea T, Nutt SR. Out-time effects on cure kinetics and viscosity for an out-of-autoclave (OOA) prepreg: Modelling and monitoring. Compos Sci Technol 2014;100:63–9. doi:10.1016/j.compscitech.2014.05.027.
22. West BPVAN, Pipes RB. The Consolidation of Commingled Thermoplastic 1971.
23. Howard S. Evaluating Consolidation Dynamics - Study of Key Consolidation Parameters in a Vacuum Bag Only (VBO) Cure. Proc. SAMPE 2016 Tech. Conf., Long Beach, CA: 2016.
24. Tavares SS, Michaud V, Månson JAE. Through thickness air permeability of prepregs during cure. Compos Part A Appl Sci Manuf 2009;40:1587–96. doi:10.1016/j.compositesa.2009.07.004.
25. Kratz J. Transport Phenomena in Vacuum Bag Only Prepreg Processing of Honeycomb Sandwich Panels. McGill University, 2013.
26. Wisnom MR, Reynolds T, Gwilliam N. Reduction in Interlaminar Shear Strength by Discreate and Distributed Voids 1996;3538:93–101.
27. Nikishkov Y, Seon G, Makeev A. Structural analysis of composites with porosity defects based on X-ray computed tomography 2014. doi:10.1177/0021998313494917.
28. Grunenfelder LK, Dills A, Centea T, Nutt S. Effect of prepreg format on defect control in out-of-autoclave processing. Compos Part A Appl Sci Manuf 2017;93:88–99. doi:10.1016/j.compositesa.2016.10.027.
29. Schechter SGK, Centea T, Nutt SR. Polymer film dewetting for fabrication of out-of-autoclave prepreg with high through-thickness permeability. Compos Part A Appl Sci Manuf 2018;114:86–96. doi:10.1016/j.compositesa.2018.08.002.

Tables:

Table 1 Summary of model parameter values

Parameters	Value	Ref.
V_f	0.74	[19]
R_{tow}	0.116 mm	Experimental
β_i	0.16	Experimental
K	6×10^{-16} m^2	[7]
Pc	1.76×10^5 Pa	[19]

Figure Captions:

Figure 1: Schematic of *in situ* monitoring method set-up

Figure 2: Void evolution in fabric prepregs during cure. Images were taken at (a) initial state, before vacuum applied, (b) 10min, (c) 36 min, (d) 1h, (e) 6 h and (f) 12 h into the cure.

Figure 3: (a) Void content, temperature, resin viscosity, and tow impregnation as a function of time. (b) Micrograph of uncured prepreg surface.

Figure 4: Void evolution under reduced vacuum conditions

Figure 5: Void content as a function of time (a) during room temperature vacuum hold and (b) during cure

Figure 6: Effects of deficient vacuum applied at different stages during cure on bubble expansion

Figure 7: (a) Model predictions of degree of impregnation as a function of time (b) Model prediction vs. experimental data.

Figure 8: Cross-sections of laminates cured at (a) 70% vacuum, (b) 80% vacuum, (c) 100% vacuum, and (d) 100% vacuum with sealed edges.

Figure 9: Interactions between inter-ply air bubbles and intra-tow air. (a-c) Expansion of inter-ply air bubbles (representative air bubbles were circled in red) , images were taken from prepreg cured at 70% vacuum at (a) 45 min, (b) 1.5h, (c) 8h; (d-f) air bubbles emerged from the pinholes, images were taken from prepreg cured at 80% vacuum at (a) 50 min, (b) 52 min, (c) 55 min into the cure

cycle; (d-f) elongated air bubbles developed alongside fiber tows. Images recorded from prepreg cured at 70% vacuum at (d) 1.5h, (b) 4h, and (f) 8h.

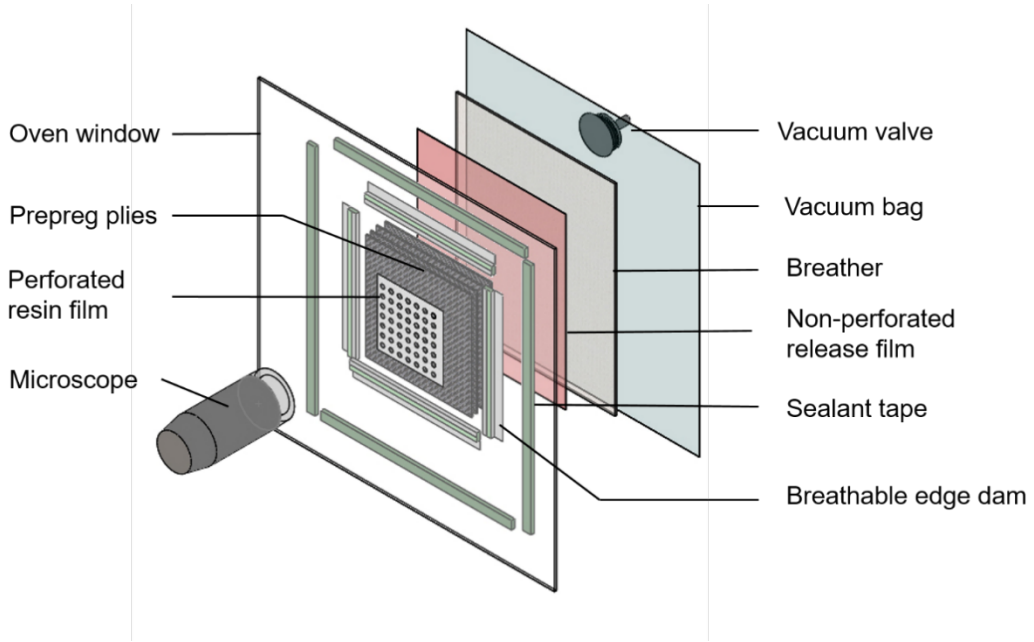

Figure 1: Schematic of *in situ* monitoring method set-up

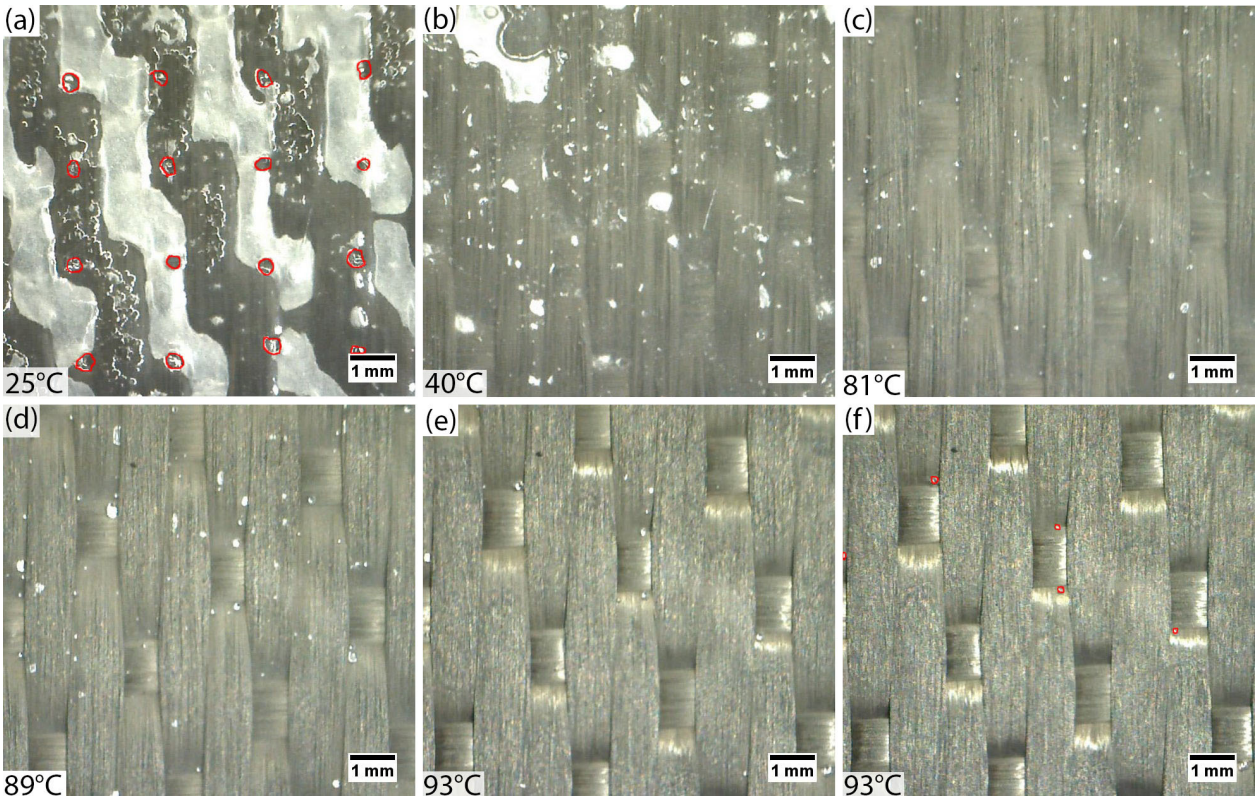

Figure 2: Void evolution in fabric prepregs during cure. Images were taken at (a) initial state, before vacuum applied, (b) 10min, (c) 36 min, (d) 1h, (e) 6 h and (f) 12 h into the cure.

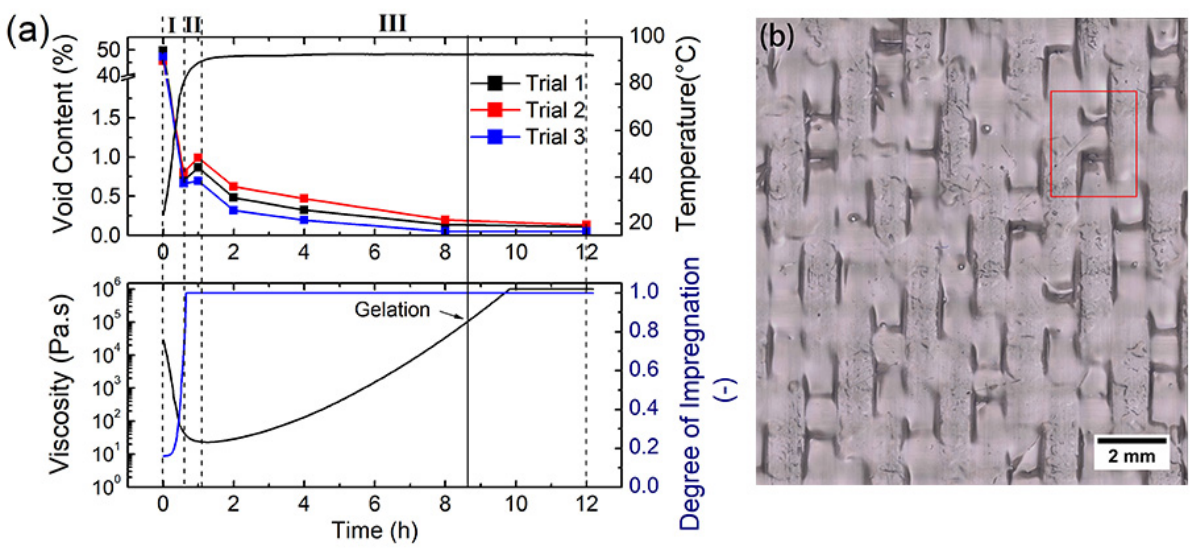

Figure 3: (a) Void content, temperature, resin viscosity, and tow impregnation as a function of time. (b) Micrograph of uncured prepreg surface.

Please cite the article as: W. Hu, Timotei Centea, Steven Nutt, **"Mechanisms of Inter-ply Void Formation during Vacuum Bag-only Cure of Woven Prepregs,"** *Polymer Compos* (2019) DOI

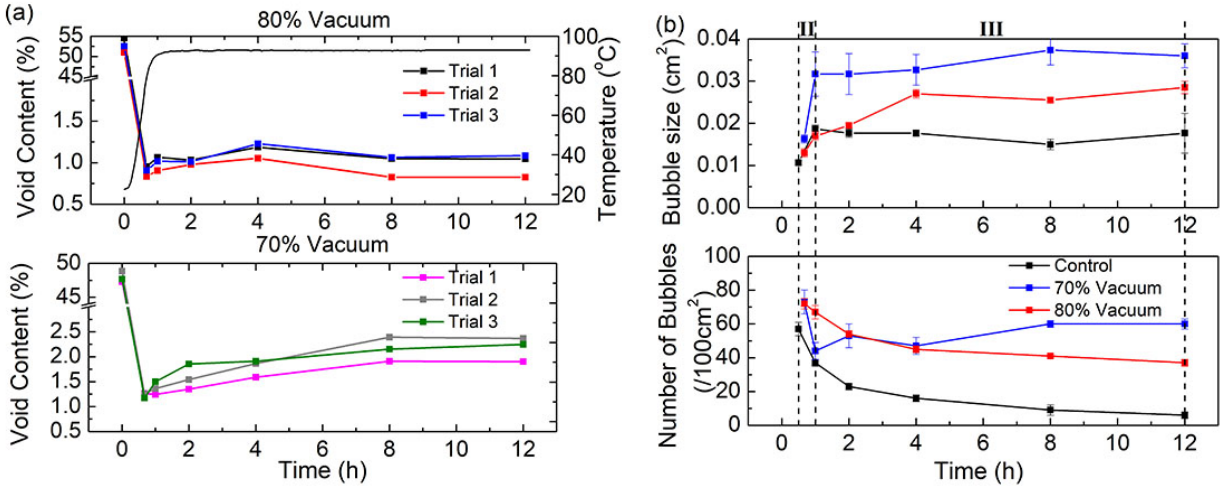

Figure 4: Void evolution under reduced vacuum conditions

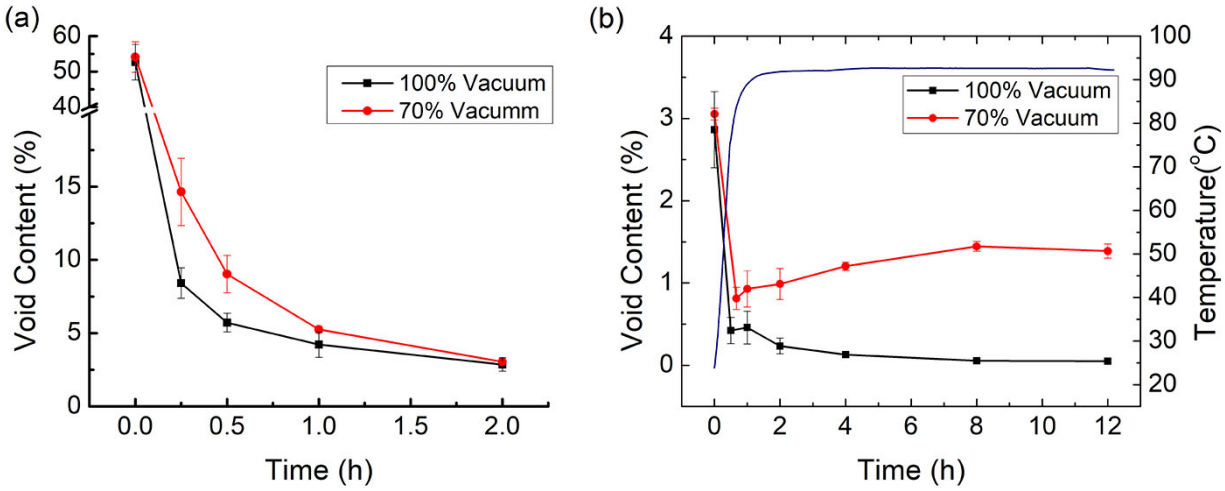

Figure 5: Void content as a function of time (a) during room temperature vacuum hold and (b) during cure

Please cite the article as: W. Hu, Timotei Centea, Steven Nutt, **"Mechanisms of Inter-ply Void Formation during Vacuum Bag-only Cure of Woven Prepregs,"** *Polymer Compos* (2019) DOI

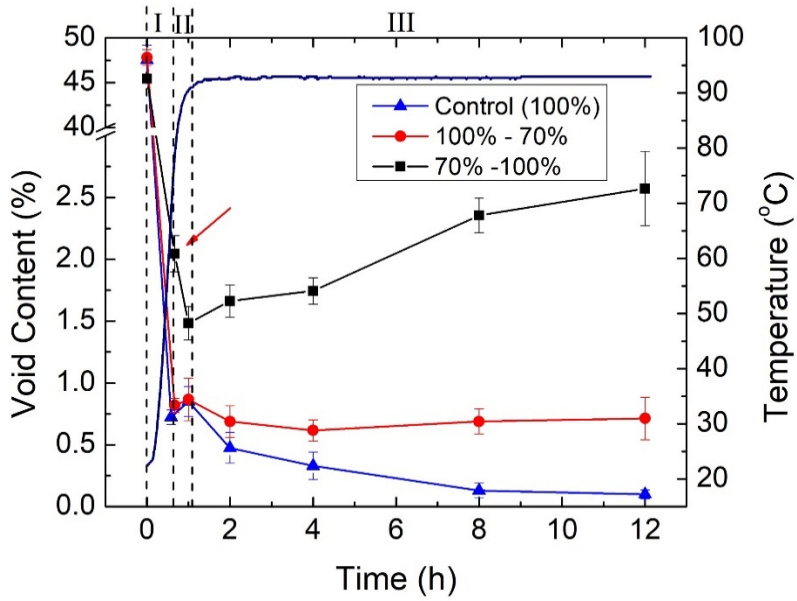

Figure 6: Effects of deficient vacuum applied at different stages during cure on bubble expansion

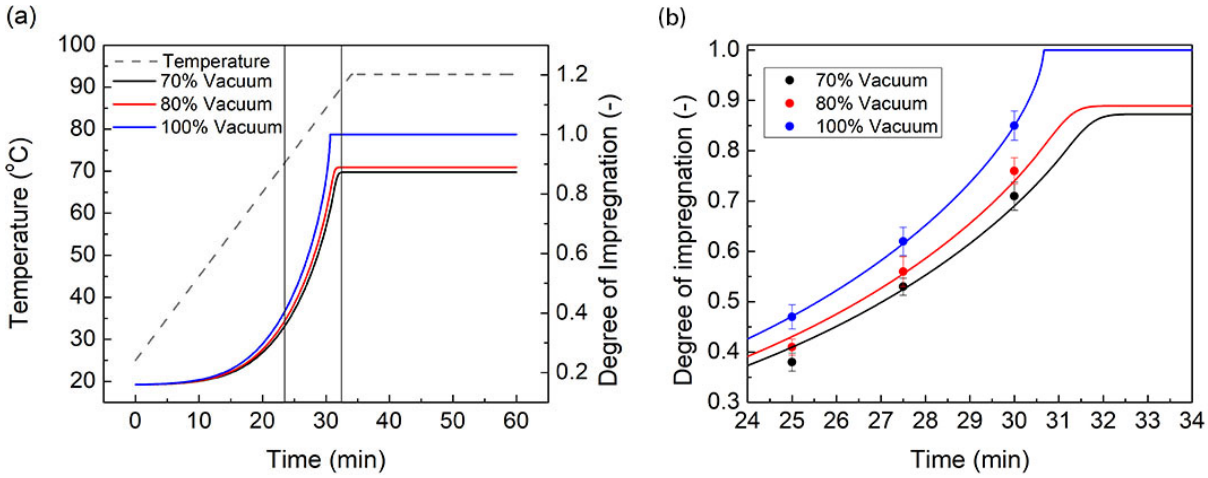

Figure 7: (a) Model predictions of degree of impregnation as a function of time (b) Model prediction vs. experimental data.

Please cite the article as: W. Hu, Timotei Centea, Steven Nutt, **"Mechanisms of Inter-ply Void Formation during Vacuum Bag-only Cure of Woven Prepregs,"** *Polymer Compos* (2019) DOI

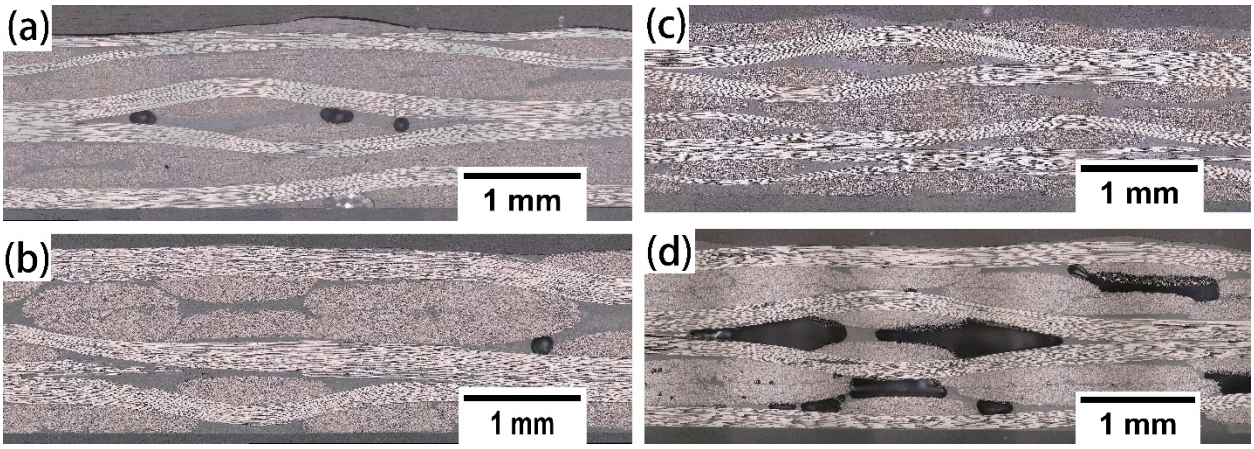

Figure 8: Cross-sections of laminates cured at (a) 70% vacuum, (b) 80% vacuum, (c) 100% vacuum, and (d) 100% vacuum with sealed edges.

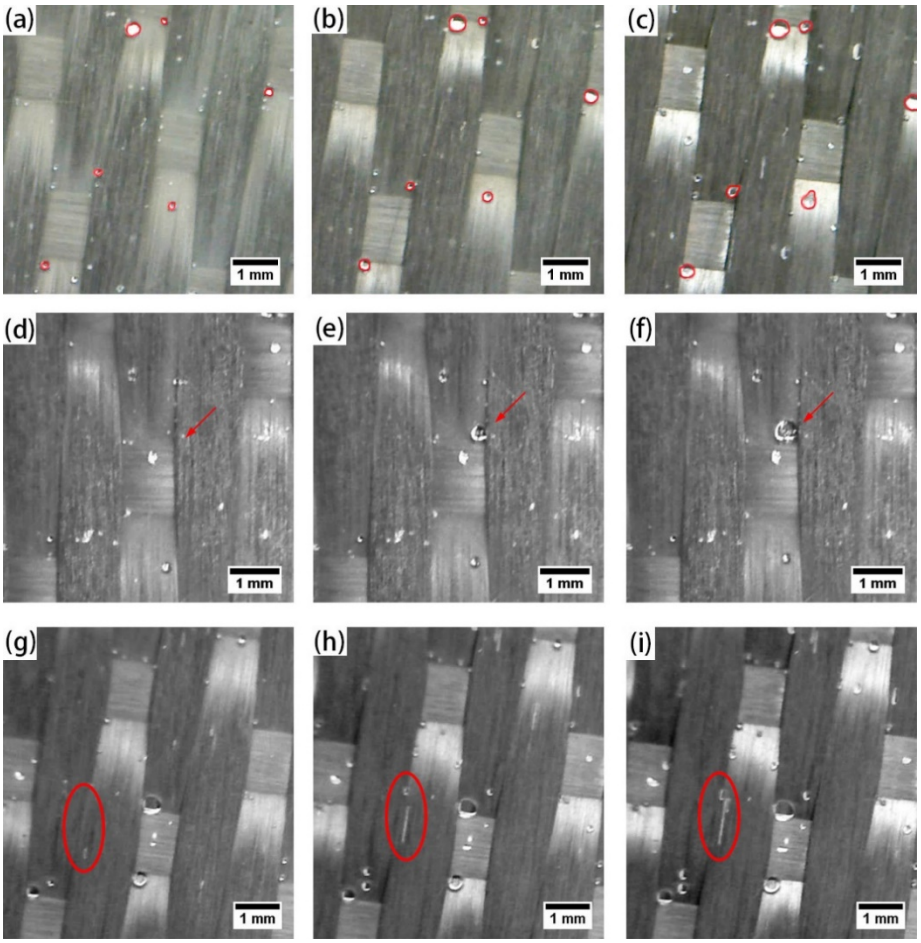

Figure 9: Interactions between inter-ply air bubbles and intra-tow air. (a-c) Expansion of inter-ply air bubbles (representative air bubbles were circled in red) , images were taken from prepreg cured

at 70% vacuum at (a) 45 min, (b) 1.5h, (c) 8h; (d-f) air bubbles emerged from the pinholes, images were taken from prepreg cured at 80% vacuum at (a) 50 min, (b) 52 min, (c) 55 min into the cure cycle; (d-f) elongated air bubbles developed alongside fiber tows. Images recorded from prepreg cured at 70% vacuum at (d) 1.5h, (b) 4h, and (f) 8h.